HHS Public Access

Author manuscript

Nat Immunol. Author manuscript; available in PMC 2017 April 01.

Published in final edited form as:

Nat Immunol. 2016 October ; 17(10): 1197–1205. doi:10.1038/ni.3554.

Follicular helper T cells progressively differentiate to regulate the germinal center response

Jason S. Weinstein[#1], **Edward I. Herman**[#2], **Begoña Lainez**[#1], **Paula Licona-Limón**[2,†], **Enric Esplugues**[2], **Richard Flavell**[2,3], and **Joe Craft**[1,2]

[1]Department of Internal Medicine (Rheumatology) Yale University School of Medicine, New Haven, CT 06520, USA

[2]Department of Immunobiology, Yale University School of Medicine, New Haven, CT 06520, USA

[3]Howard Hughes Medical Institute

[#] These authors contributed equally to this work.

Abstract

Germinal center (GC) B cells undergo affinity selection, dependent upon interactions with $CD4^+$ follicular helper T (T_{FH}) cells. We demonstrate that T_{FH} cells progressed through transcriptionally and functionally distinct stages, providing differential signals for GC regulation. They initially localized proximally to mutating B cells, secreted IL-21, induced expression of the transcription factor Bcl-6 and selected high affinity B cell clones. As the GC response evolved, T_{FH} cells extinguished IL-21 and switched to IL-4 production, showed robust CD40 ligand expression and promoted the development of antibody-secreting B cells via upregulation of the transcription factor Blimp-1. Thus, T_{FH} cells in the B cell follicle progressively differentiated through stages of localization, cytokine production and surface ligand expression to fine-tune of the GC reaction.

High-affinity antibodies and long-lived memory B cells are the hallmarks of the humoral response. Activated B cells undergo affinity maturation and differentiation in the germinal center (GC), dependent upon signals provided by $CD4^+$ follicular helper T (T_{FH}) cells[1], including interleukin 21 (IL-21) and costimulatory molecules such as CD40L (CD40 ligand) [2-5]. The signals provided by T_{FH} cells include cytokines shared by other T_H cell subsets, such as IL-4 and interferon-γ (IFN-γ), which promote B cell isotype switching

---

Address correspondence to: Joe Craft, Yale University School of Medicine, 300 Cedar ST, 541D TAC, PO Box 208031, New Haven, CT 06520-8031, joseph.craft@yale.edu.

[†]Present Addresses: Departamento de Biología Celular y del Desarrollo, Instituto de Fisiología Celular, Universidad Nacional Autónoma de México, D.F. México

AUTHOR CONTRIBUTIONS

J.S.W. and E.I.H. designed and performed experiments, and wrote the manuscript; B.L. designed and constructed the *Il21*$^{Kat/+}$ mouse and performed experiments; P.L. contributed to the design of experiments and assisted with *N. brasiliensis* infections; R.F. and E.E. assisted with the design and construction of the *Il21*$^{Kat/+}$ mouse and writing the manuscript; J.C. helped design experiments and wrote the manuscript.

The authors declare no competing financial interests.

ACCESSION CODES

Gene Expression Omnibus: GSE72568

appropriate to pathogen challenge [3,6-8]. T_{FH} cell-derived IL-21 is a key regulator of the GC as, in its absence, B cells display defects in affinity maturation and generation of long-lived plasma cells [4,5]. IL-4 also promotes the GC response as mice deficient in this cytokine or its high affinity receptor IL-4Rα have compromised immunoglobulin IgG1 and IgE responses [7,9,10], and its deletion results in defective GC B cell expansion [7]. IL-4 secretion, together with CD40-CD40L signaling, enables T_{FH} cells to induce the enzyme activation-induced cytidine deaminase (AID) in B cells, necessary for class switch recombination (CSR) and Ig affinity maturation [6,11]. The interplay of IL-21 and IL-4 signals shapes the humoral response, with IL-21-deficiency in mice resulting in increased IL-4-driven IgE switching, with their combined deficiency leading to an impairment in GC formation and antibody responses that exceeds that of either alone [12,13].

Interactive engagement between T_{FH} cells and GC B cells entails repeated short-lived cellular contacts [14]. Chronological accumulation of T cell-derived signals results in the development of B cells expressing high affinity Ig receptors [15], and their differentiation into antibody secreting cells (ASCs) [16]. Conversely, repetitive cognate T-GC B cell interactions result in TCR-dependent changes in Ca^{+} and in cytokine expression in T cells [17], with B cell-derived ICOS signals promoting proper positioning of T_{FH} cells within the B cell follicle and GC [18] and upregulation of CD40L on T_{FH} cells [19], necessary for GC B cell selection [20].

Here we show that as a consequence of T-B cell interactions, T_{FH} cell function evolved during the GC response, with these changes critical for B cell maturation. T_{FH} cells differentiated from an IL-21^{+} T_{FH} population observed proximally to the GC dark zone, the site of Ig gene hypermutation, early after immune challenge to an IL-4^{+} T_{FH} cell population robustly expressing CD40L that developed later and resided more distal to the dark zone. Modulation of the T_{FH} cell phenotype within the GC was dependent upon cell division and occurred in concert with alterations in gene expression. These distinct T_{FH} cell populations were responsible for unique effects on B cell maturation, with the IL-21^{+} T_{FH} cells enabling selection of high-affinity clones and IL-4^{+} T_{FH} cells facilitating differentiation of antibody-secreting plasma cells. Thus, after entering the GC, T_{FH} cells undergo progressive maturation to regulate GC B cell differentiation.

RESULTS

IL-4 and IL-21 expression define three populations of T_{FH} cells

Disruption of signaling by either IL-21 or IL-4 results in defective humoral responses [4,5,7,12,21]. The non-redundant functions of IL-21 or IL-4 [22] suggest that T_{FH} cells producing these cytokines are discrete, differing in their ability to regulate GC B cells. To explore this possibility, we generated C57BL/6 (B6) bicistronic *Il21-IRES-Katuska* (Kat) reporter mice (*Il21*$^{Kat/+}$) to investigate the kinetics of IL-21 expression in T_{FH} cells[17]. We immunized IL-$21^{Kat/+}$ mice intraperitoneally (i.p.) with sheep red blood cells (SRBCs)[23]. The percentage of T_{FH} cells expanded following immunization (**Supplementary Fig. 1a**), with *Il21*-Kat expression largely restricted to the follicle and absent from sites of nascent T_{FH} cell-DC interactions [24] in the T cell zone **(Supplementary Fig. 1b)**, suggesting that initial cytokine expression depended upon B cell interactions. The number of *Il21*-Kat^{+} T_{FH}

cells within the GC increased through day 12 (**Supplementary Fig. 1c**), indicating that T_{FH} cells acquire expression of IL-21 after entering the GC or that a *Il21*-Kat^{+} T_{FH} cell population entered the GC and displaced the *Il21*-Kat^{-} T_{FH} cells.

We next crossed *Il21*$^{Kat/+}$ to *Il4-IRES*-GFP (*Il4*$^{GFP/+}$; 4get) mice [25] to obtain *Il21*$^{Kat/+}$*Il4*$^{GFP/+}$ double reporter mice[17] and examined *Il21*-Kat and *Il4*-GFP expression during T_{FH} cell development. We subcutaneously (s.c.) infected *Il21*$^{Kat/+}$*Il4*$^{GFP/+}$ mice with the helminth *Nippostrongylus brasiliensis*, which induces IL-4 production in T_{FH} cells [26]. We assessed *Il21*-Kat and *Il4*-GFP expression in splenic CD4^{+}CD44^{hi}CXCR5^{hi}PD-1^{hi} T_{FH} and CD4^{+}CD44^{hi}CXCR5^{lo}PD-1^{lo} T_H2 cells, as well as in a CD4^{+}CD44^{hi}CXCR5^{int}PD-1^{int} population (**Fig. 1a**), a mixture of central memory T cells, T_H2 and pre-T_{FH} cells [27]. Three days post-parasite challenge, we detected small numbers of splenic *Il21*-Kat^{+}, *Il21*-Kat^{+}*Il4*-GFP^{+} double positive and *Il4*-GFP^{+} T_{FH} cells (**Fig. 1b**), and a fourth population that was *Il21*-Kat^{-}*Il4*-GFP^{-} double negative. From days 3 to 5, the total number of T_{FH} cells rose, driven by expansion of the *Il21*-Kat^{+} and *Il21*-Kat^{+}*Il4*-GFP^{+} pools (**Fig. 1b,c**). From day 5, *Il21*-Kat^{+} T_{FH} cells decreased, while *Il4*-GFP^{+} T_{FH} cells increased, becoming dominant by day 15, at which point the *Il21*-Kat^{+}*Il4*-GFP^{+} double positive population had also receded (**Fig. 1b**). All three populations were present in the GC at days 7-8 (**Fig. 1b,d**). By contrast, beginning at day 3, and extending to day 15 post-infection, T_H2 cells were *Il21*-Kat^{-}*Il4*-GFP^{+} as expected (**Fig. 1b**). The latter cells arose by day 3 and showed a gradual loss of *Il21*-Kat^{+} cells by day 15.

The immune response to *N. brasiliensis* begins in lymph nodes (LNs) of the mediastinum, followed by those in the mesentery, and then the spleen [28]. In the mediastinal LNs of *Il21*$^{Kat/+}$*Il4*$^{GFP/+}$ infected mice, the earliest T_{FH} cells appeared at day 2 and were mostly *Il21*-Kat^{+}; by days 3 and 5 most T_{FH} cells were *Il21*-Kat^{+}*Il4*-GFP^{+} double positive (**Supplementary Fig. 2a**). In the mesenteric nodes of infected *Il21*$^{Kat/+}$*Il4*$^{GFP/+}$ mice, T_{FH} cells were *Il21*-Kat^{+} by day 3, followed by a shift towards *Il4*-GFP^{+} T_{FH} cells by day 8 (**Supplementary Fig. 2b**), analogous to the spleen. Because we could detect GC B cells in the mediastinal and mesenteric LNs of uninfected mice (**Supplementary Fig. 2c**), presumably due to environmental antigen exposure [29], we focused the remainder of our experiments on splenic responses to minimize background.

We next assessed the cell division-dependent expression of *Il21* and *Il4* following transfer of CellTrace Violet® dye labeled ovalbumin (OVA)-specific Thy1.2^{+}CD4^{+}OT-II TCR transgenic T cells from *Il21*$^{Kat/+}$*Il4*$^{GFP/+}$ mice into congenic Thy1.1^{+} recipient mice. One day following cell transfer recipients were s.c. infected with *N. brasiliensis* combined with 4-hydroxy-3-nitrophenylacetyl-OVA (NP-OVA), followed by a single intravenous (i.v.) injection of NP-OVA two days post-infection, to ensure Ag persistence and enable tracking of Ag-specific T and B cells. *Il21*-Kat expression in the Thy1.1^{+}CD4^{+}CD44^{hi}CXCR5^{hi}PD-1^{hi} transferred T_{FH} cells was detected by the third division, while *Il4*-GFP expression was seen beginning at the fifth division, and occurred in cells that were also *Il21*-Kat^{+} (**Fig. 1e**). Three days following *N. brasiliensis* plus NP-OVA injection we found *Il21*-Kat expressing Thy1.1^{+}CD4^{+}CD44^{hi}CXCR5^{hi}PD-1^{hi} T_{FH} cells without significant expression of *Il4*-GFP (**Supplementary Fig. 3)**. These results suggest that cytokine transcript expression in T_{FH} cells occurred in a progressive manner, with *Il21*-

Kat appearing first at day 3, followed by *Il4*-GFP five days post-infection, after which *Il21*-Kat expression was gradually lost with *Il4*-GFP expression maintained to day 15.

We next sought to address the secretion of IL-4 and IL-21 proteins in reporter expressing T_{FH} cells following *N. brasiliensis* infection. Although we detected three T_{FH} cell populations expressing *Il4* and *Il21* mRNA between days 5 and 8 during our initial time-course experiment, intracellular cytokine staining after *ex vivo* stimulation with phorbol 12-myristate 13-acetate and ionomycin at these time points indicated that T_{FH} cells primarily produced either IL-4 or IL-21 (**Supplementary Fig. 4a**). Similar observations were made after i.p. immunization of wild type mice with NP-keyhole limpet hemocyanin (NP-KLH) in alum (**Supplementary Fig. 4b,c**). Using a dual-color ELISPOT assay we detected IL-21 or IL-4 protein secretion by individual splenic T_{FH} cells isolated from *Il21*$^{Kat/+}$*Il4*$^{GFP/+}$ mice 8 days following *N. brasiliensis* infection (**Fig. 1f**). While ELISPOT assays only detected a relatively small number of IL-21$^+$ and IL-4$^+$ T_{FH} cells, as noted by others [30], analysis of *Il21*-Kat$^+$, *Il21*-Kat$^+$*Il4*-GFP$^+$, and *Il4*-GFP$^+$ sorted splenic T_{FH} cells revealed a strong correlation between reporter expression and cytokine secretion, with *Il21*-Kat$^+$ T_{FH} cells producing IL-21 and *Il4*-GFP$^+$ T_{FH} cells producing IL-4, substantiating fidelity of the reporters, with the majority of T_{FH} cells secreting only one or the other cytokine (**Fig. 1f**). By contrast, relatively few T_{FH} cells co-secreted IL-21 and IL-4. Thus, we designated the *Il21*-Kat$^+$ cells as T_{FH}21 and *Il4*-GFP$^+$ cells as T_{FH}4 cells. We found that the *Il21*-Kat$^+$ *Il4*-GFP$^+$ double positive T_{FH} cells produced either IL-21 or IL-4 in ELISPOTs, rarely both, suggesting that secretion of these cytokines by T_{FH} cells is largely exclusive (**Fig. 1f and Supplementary Fig. 4a,c**); thus, we designated the dual-reporter expressing *Il21*-Kat$^+$*Il4*-GFP$^+$ T_{FH} cells as T_{FH}21+4. Collectively, these results supported the idea that cytokine expression and secretion in T_{FH} cells change over the course of an infection.

T_{FH}21 and T_{FH}4 cell populations are transcriptionally distinct

To determine if the three cytokine-expressing CD4$^+$CD44^{hi}CXCR5^{hi}PD-1^{hi} T_{FH} cell populations were transcriptionally distinct, we infected *Il21*$^{Kat/+}$*Il4*$^{GFP/+}$ mice with *N. brasiliensis* and sorted splenic *Il21*-Kat$^+$, *Il21*-Kat$^+$*Il4*-GFP$^+$, and *Il4*-GFP$^+$ T_{FH} cells, as well as *Il4*-GFP$^+$ T_H2 cells at day 8 post infection (**Supplementary Fig. 5a**). Using RNA sequencing, a total of six pairwise comparisons were made between the aforementioned four populations, resulting in 1300 genes that were differentially expressed (FDR q-value < 0.05) in at least one of the pairwise comparisons, with T_H2 cells the most different compared to each population of T_{FH} cells (**Fig. 2a and Supplementary Fig. 5b**). The T_{FH}21 and T_{FH}21+4 groups were most alike, while T_{FH}4 cells shared similarities with the T_{FH}21+4 and the T_H2 populations (**Fig. 2a and Supplementary Fig. 5b**). Clustering analysis assigned each differentially expressed gene to one of four groups (**Fig. 2a and Supplementary Fig. 5c**), representing modules of *Il21*-coregulated genes, *Il4*-coregulated genes, T_{FH}-defining genes including *Sh2d1a* and *Batf*, and non-T_{FH} effector genes such as *Il2ra* and *Tbx21*. To analyze the transcriptional differences among the three T_{FH} cell populations, we examined a curated set of genes previously described to be up- or down-regulated in T_{FH} cells compared to other CD4$^+$ T^H subsets [31-33]. The T_{FH} cell-associated transcription factor genes *Batf* and *Ascl2* [33,34] were upregulated in T_{FH}21 and T_{FH}21+4 cells compared to T_{FH}4 cells, while expression of the chemokine receptor gene *Cxcr4* was higher in T_{FH} cells expressing *Il21*-

Kat compared to other two T_{FH} cell populations (**Fig. 2b,c**). Expression of *Cxcr5* and *Pdcd1* was highest in $T_{FH}21{+}4$ cells confirmed by flow cytometry staining of CXCR5 and PD-1 (**Fig. 2d**). Thus, $T_{FH}21$, $T_{FH}21{+}4$ and $T_{FH}4$ cells were transcriptionally distinct from one other.

$T_{FH}21$ and $T_{FH}4$ cells differentially localize in the GC

CXCR4 is necessary for B cell migration between the light and dark zones (LZ and DZ) of the GC [35], and differences in its expression could affect the ability of T_{FH} cells to interact with centrocytes and centroblasts, respectively [20]. Consistent with our transcriptome analysis, at day 8 following *N. brasiliensis* infection, $T_{FH}4$ cells had significantly less surface expression of CXCR4 than $T_{FH}21$ and $T_{FH}21{+}4$ cells (**Fig. 3a**), in agreement with its upregulation by Ascl2 [34] in the latter two (**Fig. 2c**). Based upon this observation, we tested whether the T_{FH} cell populations localized to different regions of the GC. Staining of splenic sections of *Il21*$^{Kat/+}$*Il4*$^{GFP/+}$ mice with CD35 detected follicular dendritic cells that mark the GC LZ [36] (**Fig. 3b**). When measuring the distance from the centers of the DZ to the T_{FH} cells of each type in that GC we observed that $T_{FH}21$ cells were located on average more proximal to the DZ than $T_{FH}4$ cells, and that $T_{FH}21$ cells migrated more efficiently than $T_{FH}4$ cells to the CXCR4 ligand CXCL12 in the dark zone, consistent with their increased CXCR4 expression, while $T_{FH}21$ and $T_{FH}4$ migrated similarly to the control chemokine CXCL13 (**Fig. 3c**) [36]. In contrast, cell-surface expression of CD40L [37], which, in combination with IL-4, promotes IgG1 switching and regulates GC B cell differentiation via CD40 signaling [2,38], was significantly enhanced on $T_{FH}4$ and $T_{FH}4{+}21$ cells compared to $T_{FH}21$ cells at day 8 after *N. brasiliensis* infection (**Fig. 3d**). Thus, $T_{FH}4$ cells expressed increased CD40L and localized more distal to the LZ of the GC than $T_{FH}21$ cells.

$T_{FH}21$ cells become IL-4 producers upon helminth challenge

We next used an adoptive-transfer model to assess the effect of $T_{FH}21$, $T_{FH}21{+}4$ and $T_{FH}4$ cells on the humoral immune response. Previous studies have shown that following adoptive transfer, $CD4^+$ T cells maintain expression of either *Il21* or *Il4* for 7 to 10 days [6,39]. $T_{FH}21$, $T_{FH}4{+}21$ or $T_{FH}4$ cells were sorted from $Thy1.2^+$ *Il21*$^{Kat/+}$*Il4*$^{GFP/+}$ mice 8 days following *N. brasiliensis* infection and 300,000 cells from each group were transferred into $Thy1.1^+$ B6 recipients bearing an irrelevant TCR transgene specific for the GP66-77 epitope of lymphocytic choriomeningitis virus (LCMV; Smarta TCR transgenics; Stg). Recipients of cell transfers were then re-infected and spleens were harvested 13 days after the secondary infection. Following transfer and re-exposure to *N. brasiliensis* we examined cytokine reporter expression by flow cytometry and protein expression by ELISPOT assays in $Thy1.2^+CD4^+CXCR5^{hi}PD\text{-}1^{hi}$ T_{FH} cells (**Supplementary Fig. 6a**). At 13 days post-secondary infection approximately 15% of the transferred *Il21*-Kat^+ T_{FH} cells retained sole expression of this transcript, while about 50% acquired *Il4*-GFP expression (**Fig. 4a,b**). Approximately 40% of the transferred *Il21*-Kat^+*Il4*-GFP^+ double positive T_{FH} cells became *Il4*-GFP-expressing $T_{FH}4$ cells, while about 10-15% retained expression of both *Il21*-Kat and *Il4*-GFP (**Fig. 4a,b**). By contrast, virtually all of the transferred *Il4*-GFP^+ T_{FH} cells that were reporter positive were *Il4*-GFP^+, with around 15% also upregulating *Il21*-Kat (**Fig. 4a,b**). Transferred *Il21*-Kat^- *Il4*-GFP^- double negative T_{FH} cells did not acquire expression

of either cytokine at the day 13 time-point (data not shown). Transferred *Il4*-GFP$^+$ expressing cells were localized more distal to the DZ compared to the *Il21*-Kat$^+$ cells (**Supplementary Fig. 6b**), consistent with their higher CXCR4 expression. Transferred T_{FH} cell subsets maintained their surface phenotype post-transfer, albeit with fewer donor $T_{FH}4$ than $T_{FH}21$ and $T_{FH}21+4$ cells in recipient spleens (**Supplementary Fig. 6c-e**). Approximately 10% of the transferred T_H2 cells were able to acquire T_{FH} cell markers, though this resulted in fewer total T_{FH} cells than when $T_{FH}21$ or $T_{FH}21+4$ were transferred [17] (**Supplementary Fig. 6d**). In a like manner, donor T_{FH} cells was maintained similar phenotypes when examined at 7 days following transfer (**Supplementary Fig. 6f-h**).

We sorted each of the three T_{FH} cell populations at 13 days post transfer and determined their IL-21 and IL-4 production by dual color ELISPOT assays. Progeny of transferred *Il21*-Kat$^+$ T_{FH} cells contained both IL-21 and IL-4 secretors with rare cells secreting both (**Fig. 4c)**. Transferred *Il21*-Kat$^+$*Il4*-GFP$^+$ double positive T_{FH} cells robustly became IL-4-secreting cells, while transferred *Il4*-GFP$^+$ T_{FH} cells retained the IL-4 single-positive phenotype (**Fig. 4c**). There was a strong correlation between cytokine reporter expression and protein secretion in all transferred T_{FH} cells, as well as a near-absence of cells secreting IL-21 and IL-4 simultaneously (**Fig. 4c**).

To determine if T_{FH} cells isolated at an early time point following pathogen challenge exhibited similar kinetics of cytokine expression, we modified our transfer model (**Supplementary Fig. 6a**) to obtain *Il21*-Kat$^+$ and *Il21*-Kat$^+$*Il4*-GFP$^+$ T_{FH} cells from five days post-infection with *N. brasiliensis* instead of day 8. There were insufficient splenic $T_{FH}4$ cells to transfer at this time point, precluding their analysis (**Fig. 5a**). *Il21*-Kat$^+$ and *Il21*-Kat$^+$*Il4*-GFP$^+$ T_{FH} cells isolated from infected donors at day 5 maintained CXCR5 and PD-1 expression in recipients after adoptive transfer (**Fig. 5b,c**). However, in contrast to *Il21*-Kat$^+$ cells isolated 8 days after infection, which largely remained *Il21*-Kat$^+$ after transfer, 40% of such cells isolated at day 5 post-infection converted into *Il4*-GFP$^+$ expressers following transfer (**Fig. 5d**). Collectively, these data indicate a model of progressive differentiation of T_{FH} cells from *Il21*-Kat-expressing cells to *Il4*-GFP-expressing cells.

$T_{FH}21$ cells and $T_{FH}4$ cells differentially regulate GC responses

We next tested the idea that T_{FH} cell populations with differential expression of IL-21, IL-4, CD40L and CXCR4 contribute to distinctive GC B cell responses. We transferred 300,000 $T_{FH}21$, $T_{FH}4+21$ or $T_{FH}4$ cells sorted from Thy1.2$^+$ *Il21*$^{Kat/+}$*Il4*$^{GFP/+}$ mice 8 days following *N. brasiliensis* infection into Thy1.1$^+$ Stg B6 recipients, with the latter re-infected and spleens harvested 13 days after the secondary infection, a time point coinciding with the peak of the GC response. Mice that received T_{FH} cells had a significant increase in the percentages and numbers of B220$^+$IgD$^-$CD95^{hi}GL-7^{hi} splenic GC B cells compared to *N. brasiliensis*-infected mice that were not recipients of adoptively transferred cells, with those receiving $T_{FH}21+4$ cells showing the greatest increase in percentages and numbers of GC B cells and average GC size, compared to recipients of $T_{FH}21$ or $T_{FH}4$ cells (**Fig. 6a,b)**. This suggested that even though the $T_{FH}21+4$ cell population consisted of T_{FH} cells that secreted

either IL-4 or IL-21, they functioned synergistically in promoting the GC response, as predicted by *in vitro* experiments [40].

Compared to $T_{FH}21$ cells, adoptively transferred $T_{FH}21$+4 and $T_{FH}4$ cells promoted IgG1 synthesis by GC B cells, with transferred $T_{FH}21$+4 cells inducing the greatest numbers of $IgG1^+$ GC B cells (**Fig. 6c**). Additionally, IgG1 production by GC B cells in mice into which we adoptively transferred IL-$4^{-/-}$ and IL-$4^{+/+}$ $T_{FH}21$ cells were similar (**Supplementary Fig. 7a**), suggesting that the minimal amount of IL-4 produced by $T_{FH}21$ cells had a negligible effect upon IgG1 synthesis, as expected. Moreover, adoptively transferred $T_{FH}21$+4 and $T_{FH}4$ cells drove more splenic ASCs to secrete IgG1 and IgE than $T_{FH}21$ cells (**Fig. 6d and Supplementary Fig. 7b**), consistent with their increased expression of IL-4 (**Fig. 4d**) and CD40L (**Fig. 3d**) [38,41]. $T_{FH}21$+4 cells also promoted the development of more $B220^{lo}CD138^+$ plasma cells than did $T_{FH}21$ cells (**Supplementary Fig. 7c**). Using an ELISA specific for *N. brasiliensis* antigens, we found no difference in the amounts of serum IgM, but significantly higher amounts of IgG1 in recipients of $T_{FH}21$+4 and $T_{FH}4$ cells than in mice transferred with $T_{FH}21$ cells, and a trend toward increased IgE production (**Fig. 6e)**. The differences in B cell and plasma cell phenotypes in recipient mice were not the result of enhanced proliferation or diminished B cell apoptosis, because BrdU uptake in GC B cells was similar among mice transferred will all the T_{FH} cell subsets (**Supplementary Fig. 7d**), while caspase 3 activity was similar in mice that received $T_{FH}21$ or $T_{FH}4$ cells (**Supplementary Fig. 7e)**.

To assess the quality of Ag-specific GC B cells generated by the T_{FH} cell subsets, we adoptively transferred $T_{FH}21$, $T_{FH}21$+4 and $T_{FH}4$ cells isolated from Thy1.2$^+$ *Il21*$^{Kat/+}$ *Il4*$^{GFP/+}$ OT-II TCR transgenic mice at day 8 post *N. brasiliensis* infection into Stg B6 recipients. Upon transfer, these mice were infected with *N. brasiliensis* and serially administered NP-OVA (**Supplementary Fig. 7f**). Thirteen days post infection we then sequenced the *Vh186.2* gene in splenic GC B cells isolated from host mice, in order to determine the occurrence of the high-affinity tryptophan to leucine point mutation at position 33 (W33L) of the V_H186.2 Ig heavy chain [42]. Although GC B cells from all three recipient groups had a similar overall frequency of mutations in their *Vh186.2* genes (**Fig. 7b**), the W33L point mutation occurred significantly more often in GC B cells taken from recipients of $T_{FH}21$ cells compared to $T_{FH}4$ cells (**Fig. 7c**), indicating that $T_{FH}21$ cells positively promote selection, rather than merely somatic mutation. While transferred $T_{FH}21$ cells promoted the formation of fewer low- as well as high-affinity anti-NP ASCs than did $T_{FH}21$+4 and $T_{FH}4$ cells (**Fig. 7d**), this was likely due to impairment in CSR **(Fig. 6c-e and Supplementary Fig. 7a,b**) rather than in affinity maturation. Conversely, recipients of $T_{FH}21$+4 and $T_{FH}4$ cells, which had fewer GC B cell clones with mutations that confer increased affinity for NP, had higher numbers of high-affinity anti-NP IgG1 and IgE ASCs than recipients of $T_{FH}21$ cells (**Fig. 6d and Supplementary Fig. 7b)**, a finding consistent with their enhanced promotion of IgG1- and IgE-secreting ASCs. Although transferred $T_{FH}21$ cells had differentiated into $T_{FH}21$+4 and $T_{FH}4$ cells and began producing IL-4 over the 13 day course of the experiment (**Fig. 4d**), they were not able to induce the phenotypic changes in GC B cells expected of IL-4^+ T_{FH} cells, such as class-switching to IgG1 (**Fig.**

6c), potentially due to the insufficient or delayed onset of IL-4 production (**Supplementary Fig. 7a**).

In addition, GC B cells in mice transferred with $T_{FH}21$ and $T_{FH}21$+4 cells expressed significantly more Bcl-6 than those receiving $T_{FH}4$ cells (**Fig. 7e**). In contrast, expression of *Prdm1*, the gene that encodes Blimp-1, was higher in GC B cells from mice transferred with $T_{FH}21$+4 and $T_{FH}4$ cells compared to those that received $T_{FH}21$ cells **(Fig. 7f)**, a finding consistent with the decrease in Ig secretion in ASCs isolated from the latter. Thus, GC B cells in mice that received $T_{FH}21$ cells had higher affinity mutations, increased Bcl6 but decreased Ig secretion compared to mice, which received $T_{FH}21$+4 and $T_{FH}4$ cells.

DISCUSSION

We propose a model of T_{FH} cell cytokine production in type 2 immune responses, in which discrete populations of IL-21$^+$ $T_{FH}21$ and IL-4$^+$ $T_{FH}4$ cells play unique roles in determining the antibody response -- B cell selection and antibody secretion, respectively, with $T_{FH}21$ cells developing into $T_{FH}4$ cells after exposure to antigen presented by GC B cells. In support of this model, previous work using *Il21*$^{Kat/+}$*Il4*$^{GFP/+}$ mice demonstrated that highly Ag-loaded GC B cells interact with T_{FH} cells to promote TCR signaling and result in changes in T_{FH} cell expression from *Il21*-Kat to *Il4*-GFP expression over the course of several hours [17]. Here we show that these transient TCR signals are mirrored by durable changes in transcriptional program, localization and surface ligand presentation that occur over several days.

One important difference between the $T_{FH}21$ and $T_{FH}4$ cell transcriptional programs seemed to be migratory regulation. GC B cells deficient in CXCR4 fail to localize to the DZ, resulting in decreased rates of somatic mutation compared to CXCR4-sufficient cells [36]. GC B cells that more robustly engage Ag, enabling its presentation to T_{FH} cells, reside longer in the DZ than the LZ, acquiring more Ig gene mutations with increased Ag affinity [20]. Our results suggest that T_{FH} cells were not evenly distributed within the GC; rather, those cells nearest the DZ were enriched for $T_{FH}21$ cells, which efficiently select high-affinity mutant B cells. CXCR4^{hi} centroblasts lose CXCR4 and migrate out into the light zone [43]. In a like manner, $T_{FH}4$ cells that developed later in the course of the helminth-induced GC response had diminished CXCR4 expression with decreased ability to migrate efficiently to CXCL12.

Our results support the critical role of T_{FH}-cell derived IL-21 in an effective humoral response [4,5,12]. In its absence, such as in mice receiving transfers of $T_{FH}4$ cells, GC B cells expressed less Bcl-6, and generated fewer CD138$^+$ plasma cells, while showing a trend in reduction of antigen-specific ASCs and serum helminth-specific IgG1 compared to recipients of $T_{FH}21$+4 cells, in which both cytokines were present. These data demonstrated that $T_{FH}21$ and $T_{FH}21$+4 cells are essential sources of IL-21, which is required for the maintenance of Bcl-6 expression in GC B cells, GC longevity and production of plasma cells [4,5].

While IL-21 is necessary factor, $T_{FH}21$ cells on their own were not fully capable of orchestrating a productive humoral response, concordant with observations that IL-21

expression is not sufficient for ASC formation [4,5,22]. $T_{FH}21$ cells were not able to mobilize high levels of CD40L, a molecule that is critical for class-switching [44] and plasma cell differentiation [38], and also mediates Bcl-6 transcription [45,46]. Furthermore, compared to $T_{FH}4$ cells, $T_{FH}21$ cells failed to induce the expression of *Prdm1* (Blimp-1) in GC B cells, which is critical for plasma cell development [2,44,47,48], and is antagonized by Bcl-6 [49]. GC B cells from recipients of $T_{FH}21+4$ cells shared traits with those from the $T_{FH}21$ group, such as more frequent high-affinity mutations and increased Bcl6 expression, and the $T_{FH}4$ group, including increased IgG1 and *Prdm1* expression, but had reduced apoptosis compared either group of single-cytokine producers, highlighting significant synergy between IL-21 and IL-4 in promoting GC responses [12,40].

We have shown that T_{FH} cells mature phenotypically and transcriptionally over the course of the GC response. These cells exist as discrete subsets, which progressively differentiate with modulation of cytokine production [17] and of their localization and surface ligand expression to fine-tune the GC reaction.

METHODS

Mice

Mice were housed in pathogen-free conditions at the Yale School of Medicine (New Haven, CT). C57BL/6J (B6), C.129-*Il4*^{tm1Lky}/J (4get), B6.PL-*Thy1*^{a}/CyJ (Thy1.1) B6.SJL-*Ptprc*^{a}*Pep3*^{b}/BoyJ (CD45.1), and B6.Cg-Tg(TcraTcrb)425Cbn/J (OT-II) B6.*Il4*^{tm1Nnt}/J animals were purchased from The Jackson Laboratory. B6.Tg(TcrLCMV)1Aox (Smarta; Stg) mice[50] were bred in-house. To examine the expression of *Il21* in T_{FH} cells, we generated B6 bicistronic *Il21-IRES-Katuska* (Kat)reporter (*Il21*$^{Kat/+}$) mice [17]. All animals were used at 6-8 weeks of age, with approval for all procedures given by The Institutional Animal Care and Use Committee of Yale University.

N. brasiliensis Infection and Detection of Serum Antibodies

Mice were injected s.c. at the base of the tail with third-stage larvae of *N. brasiliensis* (500 viable third-stage larvae/mouse) in 0.2 mL sterile PBS with 1X gentamicin (Gibco). Animals were sacrificed at time points described in the text. Antibody ELISAs for detecting anti-L5 serum antibodies were performed as previously described [21]; briefly, stage 5 adult worms (L5) were isolated from intestines of mice infected with L3 larvae 7 days earlier and homogenized. Five micrograms of lysates were used to coat microtiter plates, which were then incubated with sera, followed by anti-mouse IgG1 and IgE secondary antibodies (**Supplementary Table 2**).

Cell Transfers and Immunizations

2×10^5 T_{FH} or T_H2 cells, sorted by flow cytometry, or 5×10^5 $CD4^+$ ovalbumin (OVA)-specific OTII TCR transgenic T cells, were transferred to recipient mice via retro-orbital injection. Cells were labeled with CellTrace™ Violet dye according to the protocol provided by the manufacturer (Life Technologies). In certain experiments, mice were immunized i.p. with 10% SRBC (Colorado Serum) (**Supplementary Fig. 1**) or 100μg NP_{14}-KLH (Biosearch Technologies) emulsified in alum (**Supplementary Fig. 4b,c**). In others, mice

were injected with 100 μg NP_{15}-OVA (Biosearch Technologies) mixed with *N. brasiliensis* (400 third-stage larvae/mouse) s.c. 24 hours post-transfer of cells (**Fig. 1e, Fig. 7, and Supplementary Fig. 3**). Mice subsequently received an additional 100μg NP_{15}-OVA in PBS every 48 hours by i.v. injection for up to 10 days. Animals were sacrificed at different time points post infection and harvested spleens were processed for flow cytometry.

RNA and cDNA Synthesis

Sorted cell populations were processed for RNA isolation and conversion into cDNA as described previously [51]. RNA from sorted cells was extracted and purified with RNeasy Mini kit (Qiagen), according to the manufacturer's instructions. RNA purity was verified by OD 260:280 and OD 260:230 ratio analysis on a NanoDrop® ND-1000 Spectrophotometer (Thermo Scientific). cDNA was synthesized with the iScript™ cDNA Synthesis kit (Bio-Rad) according to the manufacturer's instructions.

Quantitative PCR

Real-Time PCR was set up using Brilliant II SYBR Green Master Mix™ and performed on an MX4005P Thermal Cycler™ according to manufacturer's protocols (Agilent Technologies), using primers as noted (**Supplementary Table 1**). Expression was calculated with the ΔΔxp method normalized to *Hprt*, and all measurements were performed in triplicate.

Flow Cytometry and Cell Sorting

Tissues were homogenized by crushing with the head of a 1mL syringe in a petri dish followed by straining through a 40μm nylon filter. ACK buffer was used for red cell lysis and remaining cells were counted. Antibodies used for flow cytometry staining are listed in **Supplementary Table 2**. BrdU was administered to recipient mice (1.5 mg BrdU) i.p. 4 h prior to sacrifice or added daily (0.8mg/mL) in 20% sucrose drinking water for 7 days. Isolated splenocytes were stained using the BrdU staining kit (BD Biosciences) following the manufacturer's protocol. Staining for caspase 3 was performed using Caspase 3 staining kit (AAT Bioquest, Inc) following the manufacturer's protocol. Staining for CXCR5 was performed at room temperature (25°C) with 30 min incubation. Gates for T_{FH} cells (CXCR5 and PD-1) were determined in all instances based upon staining of these markers in $CD44^{lo}$ naïve CD4 T cells; *i.e.*, the top of the CXCR5 and PD-1 gates for naïve T cells were set as the bottom of that for T_{FH} cells. Intracellular staining for cytokines was performed using Cytofix/Cytoperm™ kits (BD Biosciences) following the manufacturer's protocol. Stained and rinsed cells were analyzed using an LSRII Multilaser Cytometer (BD Biosciences). For experiments requiring sorting, $CD4^+$ T cells were enriched using a biotin-based magnetic separation kit (EasySep™, StemCell Technologies) prior to cell surface staining, with specific populations sorted using a FACSAria™ (BD Biosciences). CD40L surface mobilization we performed as previously described [37]. Briefly, cells were blocked with anti-FcγRII/III antibody, and 10 μg/mL APC-labeled anti-CD40L was introduced into the cell culture immediately before stimulation PMA (50ng/mL) and ionomycin (1μg/mL) (Sigma-Aldrich), and then incubated for 30 minutes at 37°C. After 3 washes, cells were surface stained to identify subsets of $CD4^+$ T cells.

Microscopy

Spleens were snap frozen in OCT tissue-freezing solution and stored at −80°C. Tissues were cut into 8μm sections and processed as described previously [52]. Reagents used to stain sections are listed in **Supplementary Table 2**. Images were obtained from a laser-scanning confocal microscope (Model 510 META; Carl Zeiss) at 25x magnification. ImageJ software from the National Institutes of Health was used for the measurement of GC and B cell follicle size, distance measurements, and for T cell counting. The latter analyses were performed by in a blinded manner. The distance from GC T_{FH} cells to the dark zone (DZ) centers was normalized to the equivalent radius of the DZ.

Transwell Migration Assays

Chemotaxis assays were performed as described previously [53]. 5×10^5 enriched CD4 splenic T cells were incubated for 1 h with 1× DMEM containing 0.5% fatty acid–free BSA (EMD Biosciences), 5% antibiotics, L-glutamine (Cellgro), and Hepes. Cells were then allowed to migrate through 5-μm-pore–sized transwells (Corning) toward soluble CXCL12, CXLC13 (R&D Systems) or media alone, for 3 h at 37°C. Cells were collected, stained, and resuspended in 45 μl of staining buffer and analyzed by flow cytometry.

ELISPOT for Total Immunoglobulins

Splenocytes from mice infected with *N. brasiliensis* were harvested, analyzed by flow cytometry to determine B cell numbers (anti-CD19), and plated (1×10^5 cells/well) in quadruplicate on MultiScreen HTS plates (Millipore) coated with rat IgG anti-mouse light chain Abs, NP_6-BSA, or NP_{33}-BSA (Biosearch Technologies, 20 μg/ml). Antibodies used are listed in **Supplementary Table 2**. Spots were developed with Vector Blue (Vector Laboratories), and quantified using an ImmunoSpot analyzer (Cellular Technology Limited).

Cytokine ELISPOT Assays

MultiScreen HTS plates were coated overnight at 4°C with anti-IL-21 and/or anti-IL-4 (eBioscience). Sorted cells were cultured (0.25×10^5 cells/well) with PMA (50ng/mL) and ionomycin (1μg/mL) for 36 h at 37°C followed by adding primary then secondary detection antibodies (**Supplementary Table 2)**. Spots were developed with Vector Blue (Vector Laboratories) and AEC (BD Biosciences). Spots were quantified using an ImmunoSpot analyzer (Cellular Technology Limited).

Sequence Analysis of the *Vh186.2* Heavy Chain Ig Gene of NP-specific GC B Cells

GC B cells were harvested from spleens of recipient mice 13 days post infection. PCR was performed as previously described [54]. Briefly, the cDNA mixture was processed through two separate sets of the PCR reactions using Phusion high-fidelity Taq (0.02 U/μl/reaction) (Finnzymes). PCR products were cloned by zero blunt TOPO cloning (Invitrogen) and DNA sequence analysis was carried out on an Applied Biosystems 3730 capillary instrument.

RNA-Seq and Analysis

T_{FH} populations were sorted by flow cytometry. Two separate sorts were performed on different days, pooling spleens of 25-30 mice each day. Quality verification, library

preparation, and sequencing were performed at the Yale Center for Genomic Analysis. Samples were sequenced on an Illumina HiSeq 2000 using 75-bp paired end reads. Reads were aligned to the mm9 mouse genome using TopHat version 2.0.6 and Bowtie version 1.3.0, and differential expression computed with Cufflinks version 2.0.2 [55]. Analysis of RNA-seq data was done using the CummeRbund package version 2.0.0 in R. Differentially expressed genes were filtered by keeping transcripts with at least 1 read from each population significant at FDR-adjusted p-value < 0.05 between 2 of the populations, and Fragments Per Kilobase of transcript per Million mapped reads (FPKM) were summed across isoforms to obtain data for 1300 significant genes. Clustering was done using either hierarchical clustering in R by the "average" method or the partitioning around medoids method with an arbitrary value of k=4, and Jensen-Shannon distance metrics. For heatmaps, expression values were normalized per gene.

Statistics

Data were analyzed using the Student's t-test or Fisher's exact test with Prism 6 (GraphPad Software). The number of asterisks represents the degree of significance with respect to p value, with the exact value presented within each figure legend.

Supplementary Material

Refer to Web version on PubMed Central for supplementary material.

ACKNOWLEDGEMENTS

The authors acknowledge members of our departments for critical review of the manuscript. We also thank J. Henao-Mejia for assistance generating the *Il21*-reporter construct, L. Evangelisti and C. Hughes for generating ES cells and chimeric mice, respectively, J. Stein for help with the screening of knock-in mice, and E. Nevius and J. Pereira for assistance with migration assays. B6.Tg(TcrLCMV)1Aox (Smarta; Stg) mice were provided by S. Kaech (Yale University) J.S.W. was supported in part by an Arthritis Foundation Fellowship and National Institutes of Health (NIH) grant 5 T32 AR07107 and K01AR067892, and E.I.H. by NIH grants T32GM07205 and F30HL120497. Other support came from NIH (NIAMS) grants R37AR40072, P30AR053495, and R21AR063942, and the Alliance for Lupus Research (all J.C.). R.A.F. is an investigator of the Howard Hughes Medical Institute.

References

1. King C, Tangye SG, Mackay CR. T follicular helper (TFH) cells in normal and dysregulated immune responses. Annu Rev Immunol. 2008; 26:741–766. [PubMed: 18173374]
2. Xu J, Foy TM, Laman JD, Elliott EA, Dunn JJ, Waldschmidt TJ, et al. Mice deficient for the CD40 ligand. Immunity. 1994; 1(5):423–431. [PubMed: 7882172]
3. Zaretsky AG, Taylor JJ, King IL, Marshall FA, Mohrs M, Pearce EJ. T follicular helper cells differentiate from Th2 cells in response to helminth antigens. J Exp Med. 2009; 206(5):991–999. [PubMed: 19380637]
4. Zotos D, Coquet JM, Zhang Y, Light A, D'Costa K, Kallies A, et al. IL-21 regulates germinal center B cell differentiation and proliferation through a B cell-intrinsic mechanism. J Exp Med. 2010; 207(2):365–378. [PubMed: 20142430]
5. Linterman MA, Beaton L, Yu D, Ramiscal RR, Srivastava M, Hogan JJ, et al. IL-21 acts directly on B cells to regulate Bcl-6 expression and germinal center responses. J Exp Med. 2010; 207(2):353–363. [PubMed: 20142429]
6. Reinhardt RL, Liang HE, Locksley RM. Cytokine-secreting follicular T cells shape the antibody repertoire. Nat Immunol. 2009; 10(4):385–393. [PubMed: 19252490]

7. King IL, Mohrs M. IL-4-producing CD4+ T cells in reactive lymph nodes during helminth infection are T follicular helper cells. J Exp Med. 2009; 206(5):1001–1007. [PubMed: 19380638]
8. Yusuf I, Kageyama R, Monticelli L, Johnston RJ, DiToro D, Hansen K, et al. Germinal Center T Follicular Helper Cell IL-4 Production Is Dependent on Signaling Lymphocytic Activation Molecule Receptor (CD150). J Immunol. 2010; 185(1):190–202. [PubMed: 20525889]
9. Kuhn R, Rajewsky K, Muller W. Generation and analysis of interleukin-4 deficient mice. Science. 1991; 254(5032):707–710. [PubMed: 1948049]
10. Fairfax KC, Everts B, Amiel E, Smith AM, Schramm G, Haas H, et al. IL-4-secreting secondary T follicular helper (Tfh) cells arise from memory T cells, not persisting Tfh cells, through a B cell-dependent mechanism. J Immunol. 2015; 194(7):2999–3010. [PubMed: 25712216]
11. Dedeoglu F, Horwitz B, Chaudhuri J, Alt FW, Geha RS. Induction of activation-induced cytidine deaminase gene expression by IL-4 and CD40 ligation is dependent on STAT6 and NFkappaB. Int Immunol. 2004; 16(3):395–404. [PubMed: 14978013]
12. Ozaki K, Spolski R, Feng CG, Qi CF, Cheng J, Sher A, et al. A critical role for IL-21 in regulating immunoglobulin production. Science. 2002; 298(5598):1630–1634. [PubMed: 12446913]
13. McGuire HM, Vogelzang A, Warren J, Loetsch C, Natividad KD, Chan TD, et al. IL-21 and IL-4 Collaborate To Shape T-Dependent Antibody Responses. J Immunol. 2015; 195(11):5123–5135. [PubMed: 26491200]
14. Allen CD, Okada T, Cyster JG. Germinal-center organization and cellular dynamics. Immunity. 2007; 27(2):190–202. [PubMed: 17723214]
15. Oprea M, Perelson AS. Somatic mutation leads to efficient affinity maturation when centrocytes recycle back to centroblasts. J Immunol. 1997; 158(11):5155–5162. [PubMed: 9164931]
16. Kallies A, Hasbold J, Tarlinton DM, Dietrich W, Corcoran LM, Hodgkin PD, et al. Plasma cell ontogeny defined by quantitative changes in blimp-1 expression. J Exp Med. 2004; 200(8):967–977. [PubMed: 15492122]
17. Shulman Z, Gitlin AD, Weinstein JS, Lainez B, Esplugues E, Flavell RA, et al. Dynamic signaling by T follicular helper cells during germinal center B cell selection. Science. 2014; 345(6200): 1058–1062. [PubMed: 25170154]
18. Xu H, Li X, Liu D, Li J, Zhang X, Chen X, et al. Follicular T-helper cell recruitment governed by bystander B cells and ICOS-driven motility. Nature. 2013; 496(7446):523–527. [PubMed: 23619696]
19. Liu D, Xu H, Shih C, Wan Z, Ma X, Ma W, et al. T-B-cell entanglement and ICOSL-driven feed-forward regulation of germinal centre reaction. Nature. 2015; 517(7533):214–218. [PubMed: 25317561]
20. Gitlin AD, Shulman Z, Nussenzweig MC. Clonal selection in the germinal centre by regulated proliferation and hypermutation. Nature. 2014; 509(7502):637–640. [PubMed: 24805232]
21. Kumamoto Y, Linehan M, Weinstein JS, Laidlaw BJ, Craft JE, Iwasaki A. CD301b(+) dermal dendritic cells drive T helper 2 cell-mediated immunity. Immunity. 2013; 39(4):733–743. [PubMed: 24076051]
22. Ozaki K, Spolski R, Ettinger R, Kim HP, Wang G, Qi CF, et al. Regulation of B cell differentiation and plasma cell generation by IL-21, a novel inducer of Blimp-1 and Bcl-6. J Immunol. 2004; 173(9):5361–5371. [PubMed: 15494482]
23. Ismail N, Bretscher PA. The Th1/Th2 nature of concurrent immune responses to unrelated antigens can be independent. J Immunol. 1999; 163(9):4842–4850. [PubMed: 10528185]
24. Weinstein JS, Bertino SA, Hernandez SG, Poholek AC, Teplitzky TB, Nowyhed HN, et al. B cells in T follicular helper cell development and function: separable roles in delivery of ICOS ligand and antigen. J Immunol. 2014; 192(7):3166–3179. [PubMed: 24610013]
25. Mohrs M, Shinkai K, Mohrs K, Locksley RM. Analysis of Type 2 Immunity In Vivo with a Bicistronic IL-4 Reporter. Immunity. 2001; 15(2):303–311. [PubMed: 11520464]
26. Shinkai K, Mohrs M, Locksley RM. Helper T cells regulate type-2 innate immunity in vivo. Nature. 2002; 420(6917):825–829. [PubMed: 12490951]
27. Pepper M, Pagan AJ, Igyarto BZ, Taylor JJ, Jenkins MK. Opposing signals from the Bcl6 transcription factor and the interleukin-2 receptor generate T helper 1 central and effector memory cells. Immunity. 2011; 35(4):583–595. [PubMed: 22018468]

28. Lawrence RA, Gray CA, Osborne J, Maizels RM. Nippostrongylus brasiliensis: cytokine responses and nematode expulsion in normal and IL-4-deficient mice. Exp Parasitol. 1996; 84(1):65–73. [PubMed: 8888733]
29. Casola S, Rajewsky K. B cell recruitment and selection in mouse GALT germinal centers. Curr Top Microbiol Immunol. 2006; 308:155–171. [PubMed: 16922090]
30. Karlsson AC, Martin JN, Younger SR, Bredt BM, Epling L, Ronquillo R, et al. Comparison of the ELISPOT and cytokine flow cytometry assays for the enumeration of antigen-specific T cells. J Immunol Methods. 2003; 283(1-2):141–153. [PubMed: 14659906]
31. Eddahri F, Denanglaire S, Bureau F, Spolski R, Leonard WJ, Leo O, et al. Interleukin-6/STAT3 signaling regulates the ability of naive T cells to acquire B-cell help capacities. Blood. 2009; 113(11):2426–2433. [PubMed: 19020307]
32. Bauquet AT, Jin H, Paterson AM, Mitsdoerffer M, Ho IC, Sharpe AH, et al. The costimulatory molecule ICOS regulates the expression of c-Maf and IL-21 in the development of follicular T helper cells and TH-17 cells. Nat Immunol. 2009; 10(2):167–175. [PubMed: 19098919]
33. Ise W, Kohyama M, Schraml BU, Zhang T, Schwer B, Basu U, et al. The transcription factor BATF controls the global regulators of class-switch recombination in both B cells and T cells. Nat Immunol. 2011; 12(6):536–543. [PubMed: 21572431]
34. Liu X, Chen X, Zhong B, Wang A, Wang X, Chu F, et al. Transcription factor achaete-scute homologue 2 initiates follicular T-helper-cell development. Nature. 2014; 507(7493):513–518. [PubMed: 24463518]
35. Allen CD, Ansel KM, Low C, Lesley R, Tamamura H, Fujii N, et al. Germinal center dark and light zone organization is mediated by CXCR4 and CXCR5. Nat Immunol. 2004; 5(9):943–952. [PubMed: 15300245]
36. Bannard O, Horton RM, Allen CD, An J, Nagasawa T, Cyster JG. Germinal center centroblasts transition to a centrocyte phenotype according to a timed program and depend on the dark zone for effective selection. Immunity. 2013; 39(5):912–924. [PubMed: 24184055]
37. Koguchi Y, Thauland TJ, Slifka MK, Parker DC. Preformed CD40 ligand exists in secretory lysosomes in effector and memory CD4+ T cells and is quickly expressed on the cell surface in an antigen-specific manner. Blood. 2007; 110(7):2520–2527. [PubMed: 17595332]
38. Bolduc A, Long E, Stapler D, Cascalho M, Tsubata T, Koni PA, et al. Constitutive CD40L expression on B cells prematurely terminates germinal center response and leads to augmented plasma cell production in T cell areas. J Immunol. 2010; 185(1):220–230. [PubMed: 20505142]
39. Luthje K, Kallies A, Shimohakamada Y, Belz GT, Light A, Tarlinton DM, et al. The development and fate of follicular helper T cells defined by an IL-21 reporter mouse. Nat Immunol. 2012; 13(5):491–498. [PubMed: 22466669]
40. Jin H, Malek TR. Redundant and unique regulation of activated mouse B lymphocytes by IL-4 and IL-21. J Leukoc Biol. 2006; 80(6):1416–1423. [PubMed: 16943384]
41. Homig-Holzel C, Hojer C, Rastelli J, Casola S, Strobl LJ, Muller W, et al. Constitutive CD40 signaling in B cells selectively activates the noncanonical NF-kappaB pathway and promotes lymphomagenesis. J Exp Med. 2008; 205(6):1317–1329. [PubMed: 18490492]
42. Weiss U, Zoebelein R, Rajewsky K. Accumulation of somatic mutants in the B cell compartment after primary immunization with a T cell-dependent antigen. Eur J Immunol. 1992; 22(2):511–517. [PubMed: 1537385]
43. Allen CD, Okada T, Tang HL, Cyster JG. Imaging of germinal center selection events during affinity maturation. Science. 2007; 315(5811):528–531. [PubMed: 17185562]
44. Kawabe T, Naka T, Yoshida K, Tanaka T, Fujiwara H, Suematsu S, et al. The immune responses in CD40-deficient mice: impaired immunoglobulin class switching and germinal center formation. Immunity. 1994; 1(3):167–178. [PubMed: 7534202]
45. Basso K, Klein U, Niu H, Stolovitzky GA, Tu Y, Califano A, et al. Tracking CD40 signaling during germinal center development. Blood. 2004; 104(13):4088–4096. [PubMed: 15331443]
46. Saito M, Gao J, Basso K, Kitagawa Y, Smith PM, Bhagat G, et al. A signaling pathway mediating downregulation of BCL6 in germinal center B cells is blocked by BCL6 gene alterations in B cell lymphoma. Cancer Cell. 2007; 12(3):280–292. [PubMed: 17785208]

47. Shapiro-Shelef M, Lin KI, McHeyzer-Williams LJ, Liao J, McHeyzer-Williams MG, Calame K. Blimp-1 is required for the formation of immunoglobulin secreting plasma cells and pre-plasma memory B cells. Immunity. 2003; 19(4):607–620. [PubMed: 14563324]

48. Minnich M, Tagoh H, Bonelt P, Axelsson E, Fischer M, Cebolla B, et al. Multifunctional role of the transcription factor Blimp-1 in coordinating plasma cell differentiation. Nat Immunol. 2016; 17(3):331–343. [PubMed: 26779602]

49. Shaffer AL, Yu X, He Y, Boldrick J, Chan EP, Staudt LM. BCL-6 represses genes that function in lymphocyte differentiation, inflammation, and cell cycle control. Immunity. 2000; 13(2):199–212. [PubMed: 10981963]

50. Oxenius A, Bachmann MF, Zinkernagel RM, Hengartner H. Virus-specific MHC-class II-restricted TCR-transgenic mice: effects on humoral and cellular immune responses after viral infection. Eur J Immunol. 1998; 28(1):390–400. [PubMed: 9485218]

51. Poholek AC, Hansen K, Hernandez SG, Eto D, Chandele A, Weinstein JS, et al. In vivo regulation of Bcl6 and T follicular helper cell development. J Immunol. 2010; 185(1):313–326. [PubMed: 20519643]

52. Odegard JM, Marks BR, DiPlacido LD, Poholek AC, Kono DH, Dong C, et al. ICOS-dependent extrafollicular helper T cells elicit IgG production via IL-21 in systemic autoimmunity. J Exp Med. 2008; 205(12):2873–2886. [PubMed: 18981236]

53. Beck TC, Gomes AC, Cyster JG, Pereira JP. CXCR4 and a cell-extrinsic mechanism control immature B lymphocyte egress from bone marrow. J Exp Med. 2014; 211(13):2567–2581. [PubMed: 25403444]

54. McHeyzer-Williams MG, McLean MJ, Lalor PA, Nossal GJ. Antigen-driven B cell differentiation in vivo. J Exp Med. 1993; 178(1):295–307. [PubMed: 8315385]

55. Trapnell C, Roberts A, Goff L, Pertea G, Kim D, Kelley DR, et al. Differential gene and transcript expression analysis of RNA-seq experiments with TopHat and Cufflinks. Nat Protoc. 2012; 7(3): 562–578. [PubMed: 22383036]

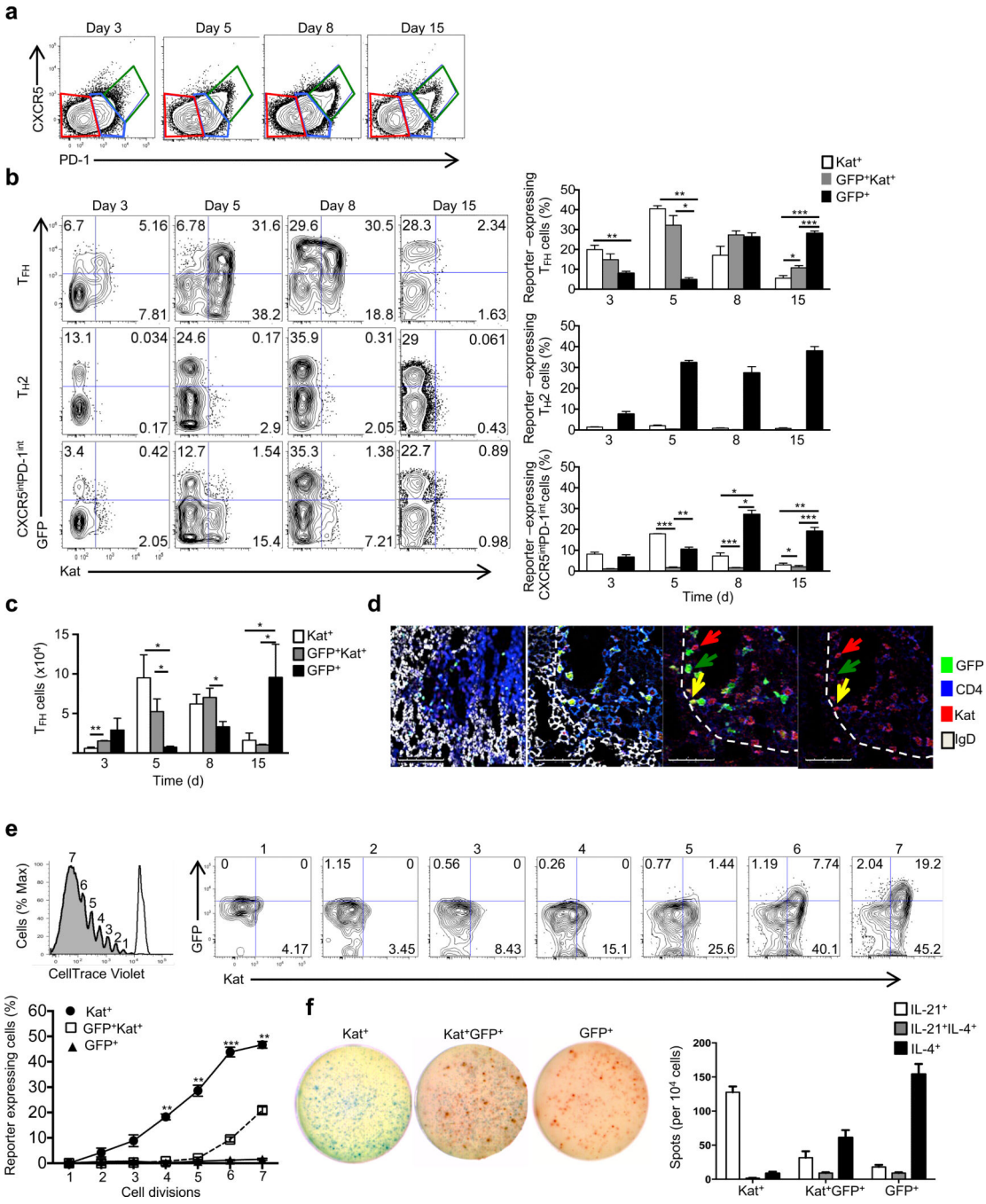

Figure 1.

Il21-Kat^{+}*Il4*-GFP^{-} T_{FH} cells transition to *Il21*-Kat^{-}*Il4*-GFP^{+} T_{FH} cells upon *N. brasiliensis* infection of *Il21*$^{Kat/+}$*Il4*$^{GFP/+}$ mice. (**a**) Flow cytometry of CD4^{+}CD44^{hi} splenocytes from *Il21*$^{Kat/+}$*Il4*$^{GFP/+}$ mice, showing CXCR5^{hi}PD-1^{hi} T_{FH} (green), CXCR5^{int}PD-1^{int} (blue), and CXCR5^{lo}PD-1^{lo} $T_{H}2$ (red) cells. (**b**) Flow cytometry of GFP (*Il4*) and Kat (*Il21*) reporter-expressing cells, gated as **a**. (**c**) Quantification of T_{FH} cells. (**d**) Confocal microscopy of GCs from *Il21*$^{Kat/+}$*Il4*$^{GFP/+}$ mice 7 days post-infection, stained with anti-GFP (green), -CD4 (blue), -Turbo635 (red), and -IgD (white) (left 2 images); anti-GFP (green), -CD4 (blue),

and -Turbo635 (red) (third image from left); and anti-CD4 (blue) and -Turbo635 (red) (far right image). Green, yellow, and red arrows indicate *Il21*$^{-}$*Il4*$^{+}$ (Kat^{-}GFP^{+}), *Il21*$^{+}$*Il4*$^{+}$ (Kat^{+}GFP^{+}), and *Il21*$^{+}$*Il4*$^{-}$ (Kat^{+}GFP^{-}) CD4^{+} cells, respectively. (**e**) Flow cytometry of CellTrace Violet labeled donor CD4^{+}Thy1.2^{+} *Il21*$^{Kat/+}$*Il4*$^{GFP/+}$ OT-II cells in Thy1.1 recipient spleens at 5 days post-infection and NP-OVA administration. Histogram showing dividing (shaded) and undivided (open; unimmunized control) donor cells (upper left) and summary of fraction of cytokine^{+} CXCR5^{+} cells among total T_{FH} cells (lower left). (**f**) Dual-color ELISPOTs of sorted reporter^{+} T_{FH} cells 8 days post-infection (as in **b**). Representative ELISPOTs (left) and total number of counted IL-21^{+} (blue), IL-4^{+} (red), and IL-21^{+}IL-4^{+} spots (purple) for each T_{FH} cell population (right). *$P < 0.05$; **$P < 0.01$; ***$P < 0.001$ (Student's *t*-test). Error bars represent standard error of the mean (SEM). Data are from one experiment representative of three independent experiments with similar results, with three or four (**a,b**), three or five (**c**), or three (**f**) mice per group.

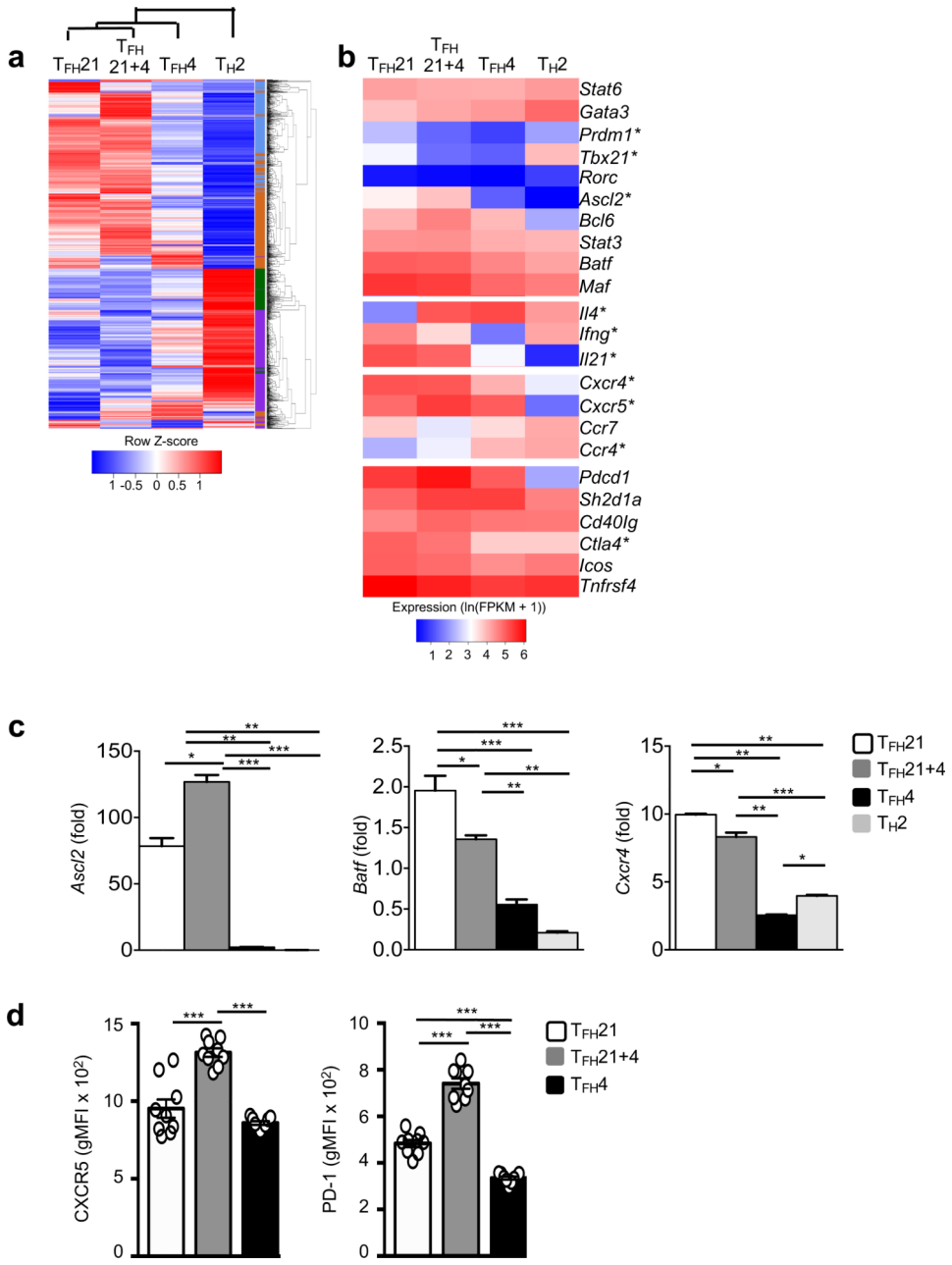

Figure 2.

Il21 and *Il4* expression define transcriptionally distinct populations of T_{FH} cells. (**a**) Heatmap of significantly ($q < 0.05$) differentially expressed genes (rows) in the four populations of cytokine expressing T_{FH} cells (columns). Light blue: cluster 1; magenta: cluster 2; light brown: cluster 3; green: cluster 4. (**b**) Heatmap of selected T cell-related genes. (**c**) Quantitative RT-PCR validation of selected genes, normalized to *Hprt*. (**d**) Flow cytometric quantification of geometric mean fluorescence intensity (gMFI) for CXCR5 and PD-1 expression from each T_{FH} cell population. * $q < 0.05$ (False discovery rate (FDR)-adjusted, comparing $T_{FH}21$ and $T_{FH}4$ cells, **b**) and * $P < 0.05$ (**c**, **d**); ** $P < 0.01$; *** $P <$ 0.001 (Student's *t*-test, **c**-**d**). Error bars represent SEM. FPKM: Fragments Per Kilobase of

transcript per Million mapped reads. Analysis utilizes data from two independent experiment with 25 and 30 mice each (**a**-**b**), is representative of two independent (of each other and of **a**-**b**) experiments performed in technical triplicates with 15 and 20 mice each (**c**), or is from one experiment representative of three independent experiments with four mice per group (**d**).

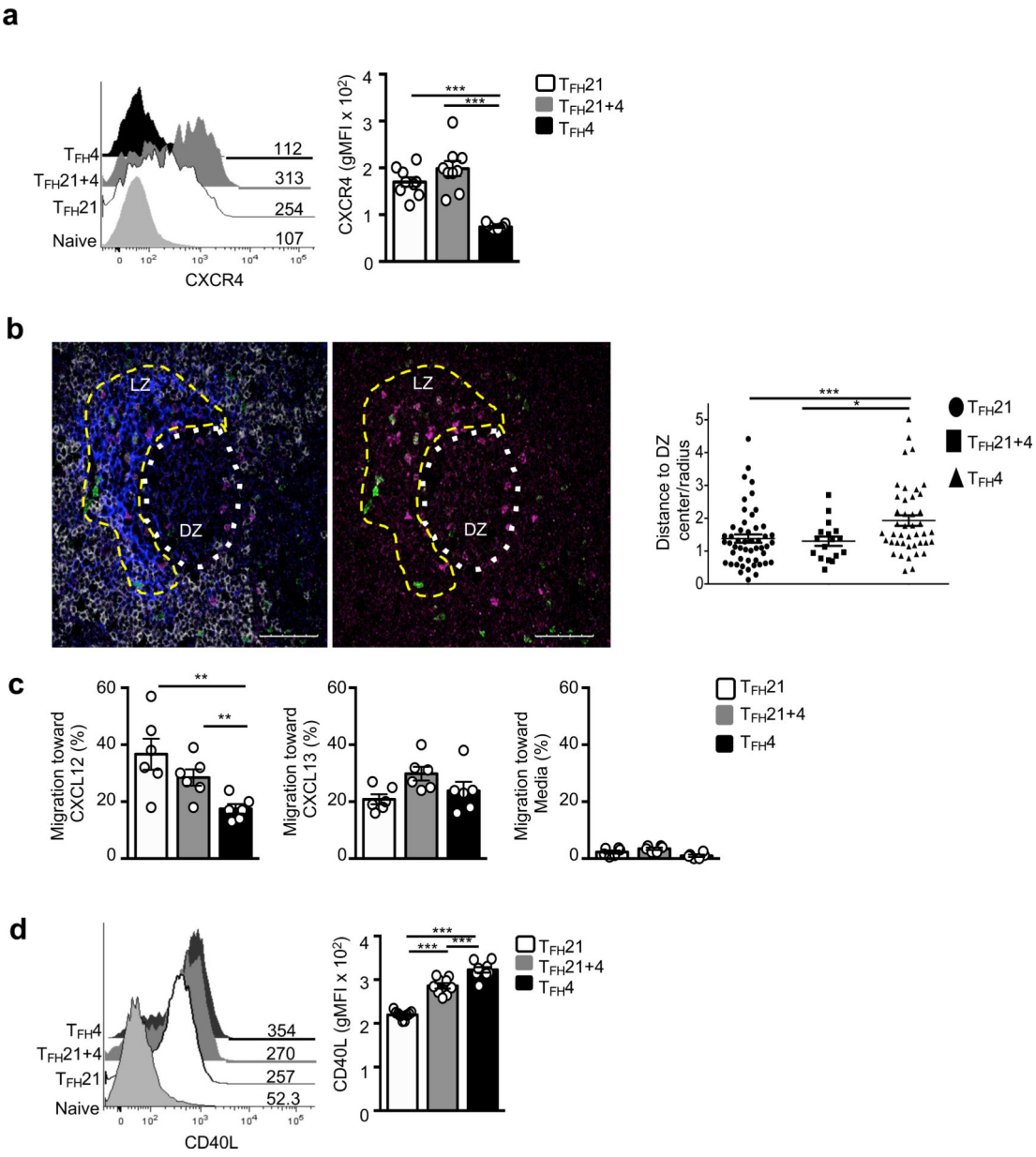

Figure 3.

$T_{FH}21$ and $T_{FH}4$ cells differentially localize in the GC with distinctive expression of CXCR4 and CD40L. (**a**) Flow cytometric quantification of CXCR4 expression in T_{FH} cell populations and naïve $CD4^+$ T cells. (**b**) Confocal microscopy of splenic GCs from *Il21*$^{Kat/+}$*Il4*$^{GFP/+}$ mice 10 days post-infection with *N. brasiliensis*, stained with anti-IgD (white), -CD35 (blue), -Turbo635 (red) and -GFP (green). (**c**) Migration assay measuring ratio of migrating to total T_{FH} cell subsets from *Il21*$^{Kat/+}$*Il4*$^{GFP/+}$ mice 8 days post-infection, co-cultured with CXCL12, CXCL13, or media, (**d**) Flow cytometric quantification of CD40L in T_{FH} cell subsets. **P*< 0.05, ***P* < 0.01; ****P* < 0.001 (Student's *t*-test, **a**,**c**,**d**). Error bars represent SEM. Data are from one experiment representative of three independent experiments (**b**-**d**), with seven (**a**), four (**b**), six (**c**), or eight (**d**) mice per group.

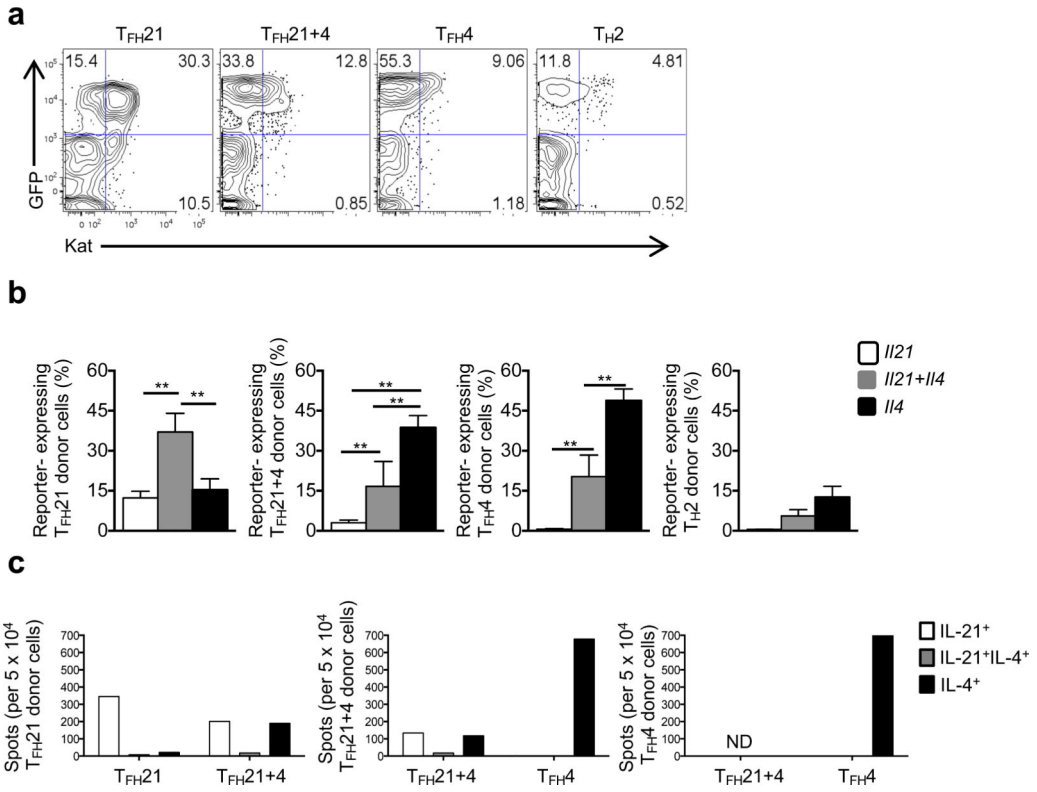

Figure 4.

T_{FH} cells modulate cytokine production after helminth infection. Flow cytometry (**a** , **b**) and dual-color IL-21 and IL-4 ELISPOT assays (**c**) of donor Thy1.2$^+$ T_{FH} cells from *Il21*$^{Kat/+}$*Il4*$^{GFP/+}$ mice at 8 days post-infection with *N. brasiliensis*, transferred into Thy1.1$^+$ Stg recipient mice and re-infected. **P* < 0.05 ***P* < 0.01 (Student's *t*-test, **b**,**c**). Error bars represent SEM. N.D.: not detected. Data are from one experiment representative of three independent experiments, with three mice per group.

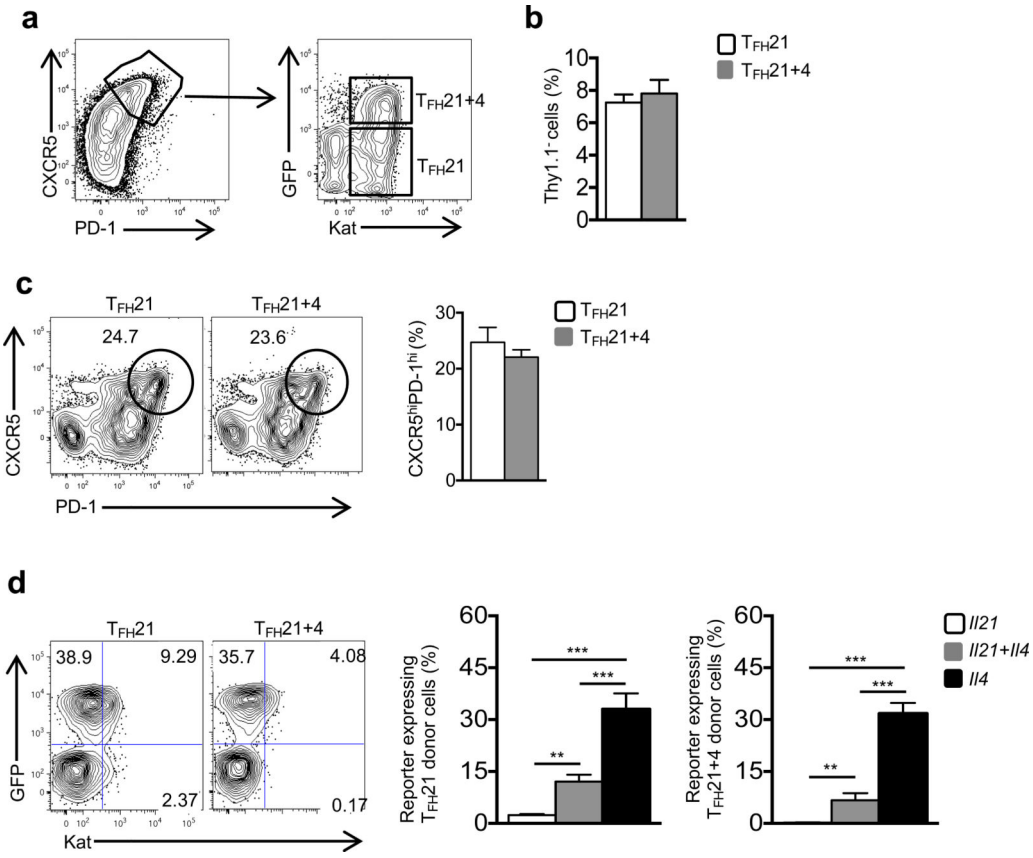

Figure 5.

T_{FH} cells transferred to Stg recipients five days after *N. brasiliensis* infection primarily become $T_{FH}4$ cells upon reinfection. (**a**, **b**) Flow cytometry of splenic donor Thy1.2$^+$ T_{FH} cells at 5 days after infection of Thy1.2$^+$ (Thy1.1$^-$) *Il21*$^{Kat/+}$*Il4*$^{GFP/+}$ mice, before transfer into Thy1.1$^+$ Stg recipients. (**c**) Flow cytometry of donor CD4$^+$Thy1.1$^-$ T_{FH} cells at 13 days after secondary infection of Thy1.1$^+$ Stg recipients. (**d**) Flow cytometry measuring GFP (*Il4*) and Kat (*Il21*) expression in donor T_{FH} cells from recipient spleens 13 days following infection (left) with percentages among donor cells (right). $^{**}P < 0.01$; $^{***}P < 0.001$ (Student's *t*-test, **d**). Error bars represent SEM. Data are from one experiment representative of three independent experiments, with four mice per group.

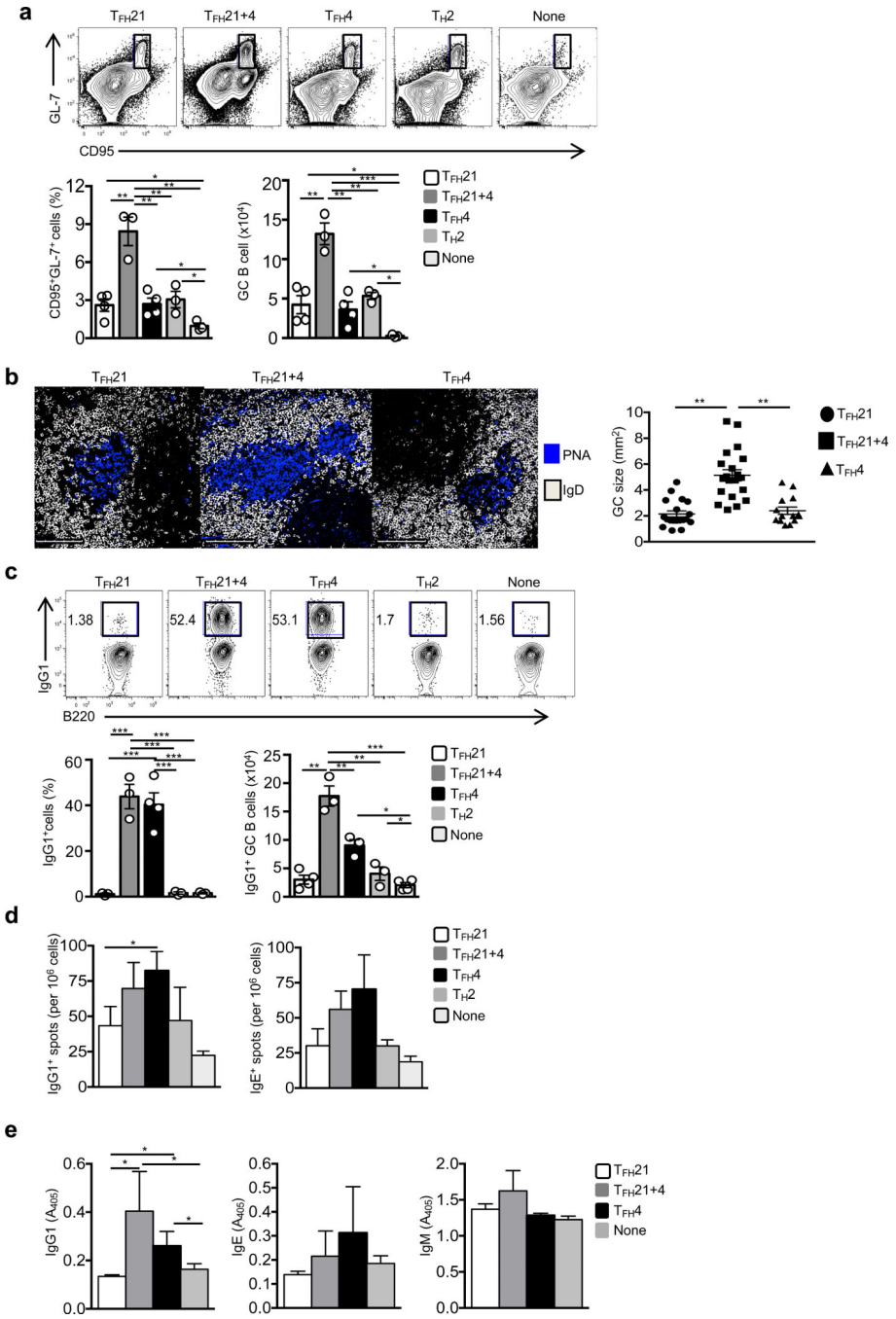

Figure 6.

Distinct T_{FH} cell populations differentially regulate the GC response. (**a**) Flow cytometry of splenic $CD4^{-}B220^{+}IgD^{lo}CD95^{+}GL\text{-}7^{+}$ GC B cells in Stg recipients at 13 days after transfer of indicated T_{FH} cells from mice infected 8 days prior with *N. brasiliensis.* (**b**) Confocal microscopy of representative splenic follicles stained with anti-IgD (white) and PNA (blue). (**c**) Intracellular flow cytometry of IgG1 in GC B cells as in (**a**). (**d**) ELISPOT assays of splenic IgG1 (top left) or IgE antibody-secreting cells (ASCs, top right) among sorted $B220^{+}$ B cells as in (**a**). (**e**) ELISA of Anti-*N. brasiliensis* IgG1 (left), IgE (middle), and IgM (right)

in sera of recipient mice. *$P < 0.05$; **$P < 0.01$; ***$P < 0.001$ (Student's *t*-test). Error bars represent SEM. Data are from one experiment representative of three independent experiments, with four mice per group.

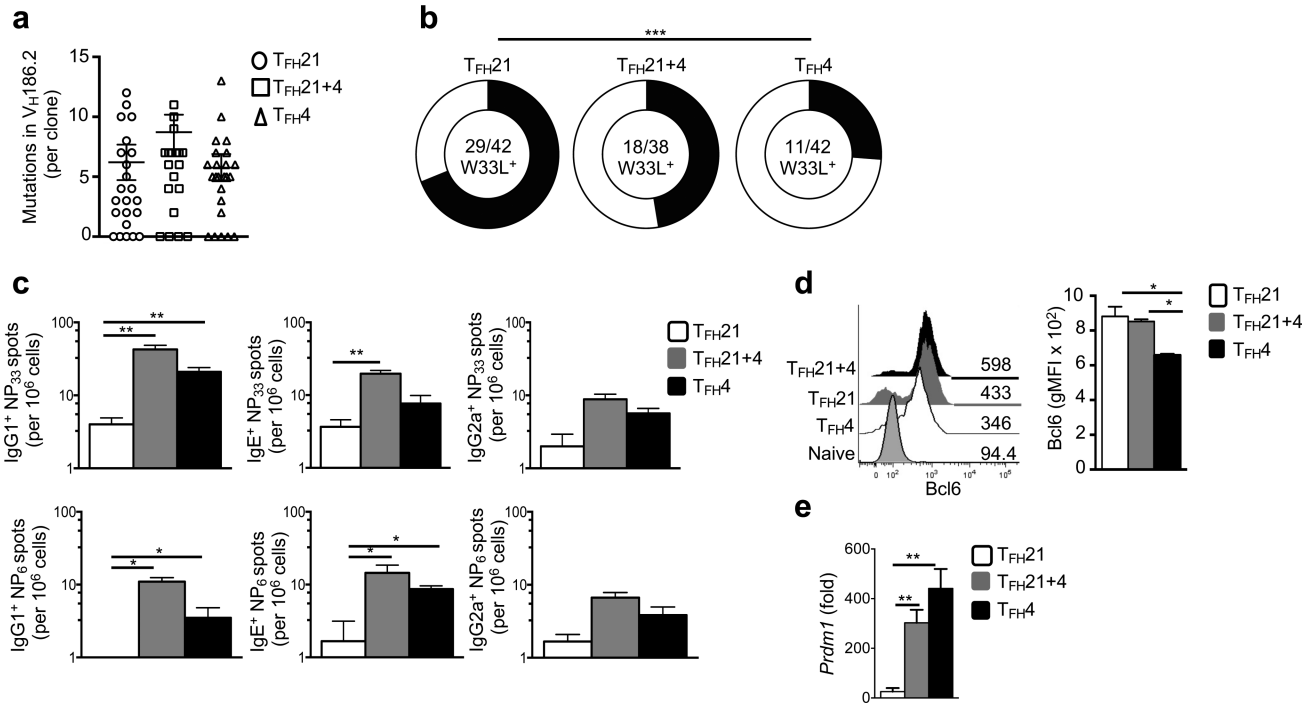

Figure 7.

$T_{FH}21$ cells promote development of higher affinity GC B cells compared to $T_{FH}4$ cells. (**a**) Total mutations (framework and complementary determining regions), and (**b**) tryptophan (W) to leucine (L) point mutations at position 33, of the $V_H186.2$ gene in sequences cloned from sorted and pooled GC B cells 13 days after administration of *N. brasiliensis* and NP-OVA with boosting to mice receiving transferred *Il21*$^{Kat/+}$*Il4*$^{GFP/+}$ OT-II$^+$ TCR transgenic T_{FH} cells (from mice infected 8 days prior with *N. brasiliensis* and NP-OVA; refer to **Supplementary Fig. 7f**) (**c**) ELISPOT assays of low (top) and high (bottom) affinity anti-NP$^+$ IgG1$^+$, IgE$^+$, or IgG2a$^+$ ASCs. (**e**) Intracellular Bcl-6 staining and (**f**) quantitative RT-PCR for *Prdm1* expression in recipient CD4−B220$^+$IgD^{lo}CD95$^+$GL-7$^+$ GC B cells after T_{FH}-cell transfer and secondary infection (as in **a**). **P* < 0.05; ***P* < 0.01; ****P* < 0.001 (Fisher's exact test (**b**) and Student's *t*-test (**c**-**e**). Error bars represent SEM. Data are from one experiment representative of three independent experiments, with four mice per group.